Predicting adsorption isotherms of organic micropollutants by high-silica zeolite mixtures

Zheng, Xinyu; Jiang, Nan; Zheng, Huaili; Wu, Yuyang ; Heijman, Sebastiaan G.J.

DOI
10.1016/j.seppur.2021.120009

Publication date
2021

Document Version
Final published version

Published in
Separation and Purification Technology

Separation and Purification Technology 282 (2022) 120009

Contents lists available at ScienceDirect

Separation and Purification Technology

journal homepage: www.elsevier.com/locate/seppur

Predicting adsorption isotherms of organic micropollutants by high-silica zeolite mixtures

Xinyu Zheng [a,b,c], Nan Jiang [a,*], Huaili Zheng [b], Yuyang Wu [b], Sebastiaan G.J. Heijman [a]

[a] Department of Water Management, Faculty of Civil Engineering and Geosciences, Delft University of Technology, P.O. Box 5048, 2600, GA Delft, the Netherlands
[b] Key Laboratory of the Three Gorges Reservoir Region's Eco-Environment, State Ministry of Education, Chongqing University, Chongqing 400045, China
[c] Department of Municipal Engineering, Suzhou University of Science and Technology, Suzhou 215009, China

ARTICLE INFO

Keywords:
High-silica zeolite mixture
Organic micropollutants
Adsorption isotherm prediction
Water treatment

ABSTRACT

One framework type of high-silica zeolite only can effectively remove a limited range of organic micropollutants (OMPs) from water. In order to extend the OMP removal range, different types of high-silica zeolites need to be combined in the adsorption process. In this study, Mordernite (MOR) and ZSM-5 (MFI) high-silica zeolite powders were mixed in different mass ratios. The removal performances of eight OMPs by zeolite mixtures, as well as single MOR and MFI zeolites, were evaluated through batch adsorption experiments to investigate their adsorption behaviors and mechanisms. When there was only one solute in water, the adsorption isotherms of OMPs by zeolite mixtures were well predicted by combining the experimental adsorption isotherms of single zeolites based on the mass ratios of single zeolites. In multi-solute water, adsorption isotherms by zeolite mixtures were calculated with less accuracy when solely combining experimental isotherms of single zeolites, especially in the case of having a lower portion of more-effective zeolite in the mixture. This could be attributed to the competition for more-effective zeolite between different OMPs.

1. Introduction

In recent years, organic micropollutants (OMPs), including pharmaceuticals, industrial additives, personal care products, herbicides, and pesticides, have been frequently detected in surface water and ground water [1]. Although the detected concentration of OMPs is generally at a trace level, i.e., a few ng L^{-1} ~ several μg L^{-1}, the persistence and accumulation of OMPs can negatively affect ecosystems. Several studies implied that OMPs discharged into water bodies will increase the antibiotic resistance of bacteria and will interfere with hormones of aquatic animals, thereby significantly threatening the health of aquatic living organisms and human beings [2-4].

Different techniques, such as adsorption [5], oxidation [6] and membrane filtration [7], are investigated as supplementary steps to remove OMPs in water treatment plants. Activated carbon adsorption is one of the most commonly used techniques for OMP removal [8]. With a high surface reactivity, a large surface area and a well-developed internal porous structure, activated carbon can adsorb a wide range of OMPs [9,10]. However, it is difficult for activated carbon to remove hydrophilic OMPs [11]. Furthermore, the adsorption efficiency of hydrophilic OMPs by activated carbon is severely affected by background organic matters (BOMs), since BOMs compete with OMPs for adsorption sites and block the pores of activated carbon [12,13].

Zeolites are microporous, crystalline aluminosilicates with orderly three-dimensional structures composed by SiO_4 and AlO_4 tetrahedrons. The properties of zeolites vary with the ratio of silica (Si) to aluminum (Al) contents (Si/Al ratio) [14]. High-silica zeolites, i.e., Si/Al molar ratio higher than five, are manufactured by replacing Al content with Si. The hydrophobic characteristic of high-silica zeolites is beneficial for OMP adsorption from aqueous solutions, since the competition of water molecules is effectively eliminated [15,16]. Moreover, zeolites only contain micropores with pore sizes less than 2.0 nm. The micropores of zeolites can exclude a majority of BOMs and promote OMP adsorption [17]. Since zeolites are chemical and thermal resistant, reuse of zeolites can be realized by both thermal and chemical regeneration [15,18,19]. One featured regeneration method for zeolites is to oxidize adsorbed OMPs by ozone, Fenton, H_2O_2 and other oxidants. Fu M. et al. has investigated the application of oxidation regeneration for zeolite granules. They found that the acetaminophen adsorption capacity recovery rate of zeolite granules remained 86% after three adsorption-regeneration cycles with ozone, which offered the possibility to on-site regenerate exhausted zeolites by ozone [20]. Because of these superior

* Corresponding author.
E-mail address: N.Jiang@tudelft.nl (N. Jiang).

https://doi.org/10.1016/j.seppur.2021.120009
Received 24 June 2021; Received in revised form 23 October 2021; Accepted 24 October 2021
Available online 27 October 2021

characteristics, high-silica zeolites are considered to be a feasible alternative to activated carbon in the removal of OMPs from water [21].

The pore size and porous structure (cages and channels) of high-silica zeolites vary by their framework types. Mordernite (MOR), ZSM-5 (MFI), Faujasite (FAU) and Beta (BEA) are the most widely used types due to their high accessible area and easy commercial availability [22]. In previous research, high-silica zeolites have been proven to exhibit excellent adsorption capabilities towards different types of OMPs, e.g., methyl tertiary-butyl ether [23], phenol [24], nicotine [25], sulfonamide [26] and so on, while zeolite with one framework type only effectively removed a limited range of OMPs. For example, Rossner et al. [27] studied the adsorption performances of 28 OMPs by FAU and MOR zeolites. At a dosage of 100 mg L^{-1}, only three OMPs were removed by FAU and 15 OMPs were removed by MOR. Ridder et al. [28] studied the removal efficiencies of 16 pharmaceuticals from demineralized water by MFI and MOR zeolites. According to their findings, nine pharmaceuticals were partially removed by MFI and 13 pharmaceuticals were removed by MOR. Only two pharmaceuticals were completely removed by both MFI and MOR. These phenomena can be explained by the close-fit theory, which suggests that the interaction between OMP and high-silica zeolite with certain framework is strong when zeolite's pore size is similar to OMP's molecular size [28,29]. In order to combat the pollution caused by increasingly diversified OMP species in water environment, different types of high-silica zeolites need to be combined in the adsorption process. To the best of our knowledge, no research has been conducted to investigate the adsorption behaviors and mechanisms of a broad range of OMPs by high-silica zeolite mixtures.

In this study, MOR and MFI were selected as the single zeolites to be combined in adsorption processes because they showed good adsorption efficiency for a range of OMPs. The pore opening size of MOR is from 2.6 Å to 7.0 Å, the wide size range is beneficial for the adsorption of different types of OMPs. While the pore opening size of MFI is around 5.0 Å, the relatively small size may provide a better adsorption capability towards OMPs with low molecular weights [15]. For example, He and Cheng [30] studied the adsorption performances of low molecular weight pollutant N-nitrosodimethylamine (MW = 74.08 g mol^{-1}) by different framework types of high-silica zeolites. They found that MFI showed a 4–7 times greater adsorption capacity than FAU and MOR at an initial N-nitrosodimethylamine concentration of 5 mg L^{-1}. For the adsorption of methyl tertiary-butyl ether at an equilibrium concentration of 1 mg L^{-1}, Erdem-Senatalar et al. [31] found that the adsorption capacity of MOR was 22 mg g^{-1}, while the adsorption capacity of BEA was 8 mg g^{-1} and the adsorption capacity of FAU was negligible. Knappe and Campos [32] also concluded that MOR and MFI zeolites were more effective than BEA and FAU zeolites in the removal process of methyl tertiary-butyl ether.

Herein, MOR and MFI high-silica zeolite powders were mixed in three different mass ratios (i.e., 4:1, 1:1 and 1:4) and served as the adsorbents to remove OMPs at an environmentally relevant concentration. A total of eight OMPs, including benzotriazole, 4-/5-methyl-benzotriazole, carbamazepine, diclofenac, metoprolol, sulfamethoxazole, propranolol and sotalol, were selected as the target OMPs, because these OMPs were recommended by the Dutch Ministry of Infrastructure and Water Management as potential guide substances to evaluate the effectiveness of OMP removal techniques. The adsorption capabilities of benzotriazole by single zeolites (i.e., MOR and MFI) and zeolite mixtures (i.e., MOR and MFI mixtures with different mass ratios) were first evaluated in single-solute water (with benzotriazole only), and then in multi-solute water (with benzotriazole and other seven OMPs). Afterwards, the adsorption performances of benzotriazole in single-solute water and multi-solute water were compared to explain the adsorption mechanisms. After that, the adsorption isotherms of zeolite mixtures towards different OMPs were calculated by combining the adsorption isotherms of single zeolites. Finally, the deviation between calculated and experimental adsorption isotherms of zeolite mixtures was discussed to examine the possible application in practice.

2. Materials and methods

2.1. Materials

MOR and MFI zeolite powders were purchased from Tosoh Corporation, the Netherlands. The characteristics of MOR and MFI zeolite powders were shown in Table 1. Their Si/Al molar ratios and pore opening sizes were obtained from the supplier. The Brønsted acid sites are weakly bound protons of a bridging hydroxyl group, typically between silica and aluminium (–Si–OH^{+}–Al–). Lewis acid sites are formed at the extra framework aluminium species and framework defects of hydrogen-type zeolites. The number of BAS and LAS in MOR and MFI zeolites was determined to represent the Al content in the framework of zeolites. The description of the procedures used for acid site measurement is given elsewhere [14].

The surface area and pore volume of zeolite powders were determined by N_2 gas adsorption (Gemini VII 2390p analyzer, Micromeritics). The N_2 adsorption isotherms of MOR and MFI zeolite powders were plotted in Figure S1. The micropore surface area and external surface area of zeolite powders were estimated by the t-plot method. Zeta potentials of MOR and MFI zeolite powders at pH 3–9 were measured to determine the charge on the external surface of zeolites. The method was described in Supplementary Information. The zeta potential-pH profiles of MOR and MFI zeolite powders were plotted in Figure S2.

MOR and MFI powders were dried at 105 °C for 24 h. Zeolite mixtures were prepared through mixing dried MOR and MFI zeolites with three MOR/MFI mass ratios, i.e., 4:1, 1:1 and 1:4, and for example, the mass ratio 4:1 meant that the weight percentages of MOR and MFI in zeolite mixture were 80% and 20%, respectively. Therefore, a total of five zeolites and zeolite mixtures were studied, namely MOR, MFI, MOR/MFI 4:1, MOR/MFI 1:1 and MOR/MFI 1:4. MOR, MFI and zeolite mixtures were dried at 105 °C for overnight and stored in the desiccator before use.

A total of eight OMPs were used in this study: Benzotriazole (BZT), 5-methyl-benzotriazole (MBZ), carbamazepine (CBZ), diclofenac (DCF), metoprolol (MTP), sulfamethoxazole (SMX), propranolol (PRO) and sotalol (STL). OMP standards (benzotriazole, 5-methyl-benzotriazole, carbamazepine, diclofenac sodium salt, metoprolol tartrate, sulfamethoxazole, propranolol hydrochloride, sotalol hydrochloride, product information in Table S1) were purchased from Sigma-Aldrich, the Netherlands. The physicochemical properties of OMPs, e.g., molecular weight, log D and charge were summarized in Table 2. The chemical structures of OMPs were shown in Figure S3.

2.2. Adsorption experiments

The stock solution of BZT was prepared by dissolving BZT standard in ultrapure water (ELGA, the Netherlands) to reach the concentration of 400 mg L^{-1}. Single-solute water was prepared by diluting BZT stock solution 100,000 times with ultrapure water to ~4 μg L^{-1}.

The stock solution of OMP mixture was prepared by dissolving OMP standards in ultrapure water for two weeks in dark with magnetic stirring. The concentration of each OMP in stock solution was approximately 1 mg L^{-1}. Multi-solute water was diluted from the stock solution of OMP mixture with ultrapure water to reach ~4 μg L^{-1} of each OMP.

Adsorption experiments were performed by dosing different amounts of zeolites and zeolite mixtures (0, 1, 2, 5, 10, 25, 50, 100 mg) to 100 ml single-solute water or multi-solute water in 100 ml Duran glass bottles. These bottles were wrapped with aluminum paper to prevent photodegradation. Zeolites and solutions were mixed at 120 rpm in an orbital shaker at 20 ± 1 degree. The adsorption time was set at 48 h to enable that the adsorption equilibrium was obtained (Figure S4). After 48 h, 1 ml solution was filtrated using a 0.2 μm regenerated cellulose syringe filter (13 mm, Whatman, Spartan), which was rinsed with 5 ml tap water and 15 ml sample solution to minimize OMP adsorption by filters. Samples were stored under 4 degree in dark for analysis.

Table 1
Characteristics of MOR and MFI zeolite powders.

Framework type	Product name	Si/Al molar ratio	BAS (μmol g^{-1})	LAS (μmol g^{-1})	Pore opening size (Å×Å)	BET surface area (m^2 g^{-1})	Micropore surface area (m^2 g^{-1})	External surface area (m^2 g^{-1})	Pore volume (cm^3 g^{-1})
MOR	690HOA	120	52	8	6.5 × 7.0 2.6 × 5.7	431	360	71	0.2687
MFI	890HOA	750	n.d.[a]	n.d.[a]	5.1 × 5.5 5.3 × 5.6	334	282	52	0.1702

a. Not detected.

Table 2
Names and physicochemical properties of OMPs.

Name	CAS No.	Formula	Molecular weight (g mol^{-1})	LogD[a]	Surface charge[a]
Benzotriazole (BZT)	95–14-7	$C_6H_5N_3$	119.1	1.30	0
5-methyl-benzotriazole (MBZ)	136-85-6	$C_7H_7N_3$	133.2	1.81	0
Carbamazepine (CBZ)	298–46-4	$C_{15}H_{12}N_2O$	236.3	2.77	0
Diclofenac (DCF)	15307–86-5	$C_{14}H_{11}Cl_2NO_2$	296.1	2.46	–
Metoprolol (MTP)	37350–58-6	$C_{15}H_{25}NO_3$	267.4	−1.39	+
Sulfamethoxazole (SMX)	723–46-6	$C_{10}H_{11}N_3O_3S$	253.3	0.65	–
Propranolol (PRO)	525–66-6	$C_{16}H_{21}NO_2$	259.3	−0.57	+
Sotalol (STL)	3930–20-9	$C_{12}H_{20}N_2O_3S$	272.4	−3.09	+

[a] At pH 5.8. Estimated by Chemicalize Platform.

2.3. LC-MS analysis

The concentrations of OMPs in sample solutions were analyzed through liquid chromatography tandem triple quadrupole mass spectrometry (LC-MS). Chromatographic separation of OMPs was performed by the ACQUITY UPLC® BEH C18 column (2.1 × 50 mm, 1.7 μm, Waters, Ireland) with gradient elution of ultrapure water and acetonitrile as the mobile phase. Ultrapure water and acetonitrile (LC-MS grade, Biosolve, France) were acidified with 0.1% formic acid (LC-MS grade, Biosolve, France). The flow rate of mobile phase was set at 0.35 ml min^{-1} using an ACQUITY UPLC I-Class Plus pump (Waters, USA). Mass spectrometry (Xevo TQ-S micro, Waters, USA) was conducted in the positive (ESI +) and negative (ESI-) electrospray ionization modes. The obtained data were analyzed by the TargetLynx software. OMP concentrations in the calibration standards ranged from 0.0025 μg L^{-1} to 10 μg L^{-1}. The detection limits of OMPs were listed in Table S2.

OMP concentrations were calculated by referring to the corresponding internal standards, which were OMP standards with isotopic elements. The names of internal standards were listed in Table S3. The internal standard mixture was prepared by mixing eight internal standards in ultrapure water. The concentration of each internal standard was ~100 μg L^{-1}. Calibration standards contained ~1 μg L^{-1} internal standards. Prior to LC-MS analysis, 495 μL filtrated samples were mixed with 5 μL internal standard mixtures to reach a total volume of 500 μL to obtain the same concentration of internal standards as in calibration standards

2.4. Adsorption model

The adsorption capacity q_e (μg mg^{-1}) of OMPs by zeolites (mixtures) was calculated with Eq. (1),

$$q_e = \frac{(C_0 - C_e) \times V}{m} \quad (1)$$

where C_0 (μg L^{-1}) and C_e (μg L^{-1}) are the initial and equilibrium concentrations of OMPs, respectively, V (L) is the volume of single-solute water/multi-solute water and m (mg) is the mass of zeolites (mixtures).

In this study, adsorption isotherm data were fitted using Freundlich model. Freundlich model is a semi-empirical equation, which assumes that the adsorption process occurs on a heterogeneous surface and the adsorbent's adsorption amount increases with the increase of adsorbate's concentration. The non-linear form of the Freundlich model was shown in Eq. (2),

$$q_e = K_F C_e^n \quad (2)$$

where K_F ((μg mg^{-1}) (μg L^{-1})$^{-n}$) and n (-) are the Freundlich constants.

3. Results and discussion

3.1. Adsorption of BZT in single-solute water

The adsorption isotherms of BZT by MOR, MFI and their mixtures accompanied by the Freundlich fitting curves were depicted in Fig. 1. The corresponding Freundlich isotherm constants were listed in Table 3. In the studied concentration range, the adsorption isotherms of BZT by MOR, MFI and zeolite mixtures were accurately described by the Freundlich model, since the R^2 values were close to 1. When n value was around 1, higher K_F value indicated higher adsorption capability [15]. Thus, the affinity between MOR and BZT (K_F = 24.4E-3) was stronger than that between MFI and BZT (K_F = 3.0E-3). As can be seen from Fig. 1, the adsorption isotherms of zeolite mixtures were in between the adsorption isotherms of single zeolites and the adsorption capacity of zeolite mixtures was related to the mass ratio of single zeolite. According to these findings, it was assumed that the adsorption of OMPs by zeolite mixtures could be described by the adsorption isotherm and mass ratio of single zeolite.

In practice, an optimal mass ratio of single zeolite will be settled for the adsorption of a broad range of OMPs by zeolite mixtures. For this purpose, it is meaningful to pre-estimate the OMP adsorption capabil-

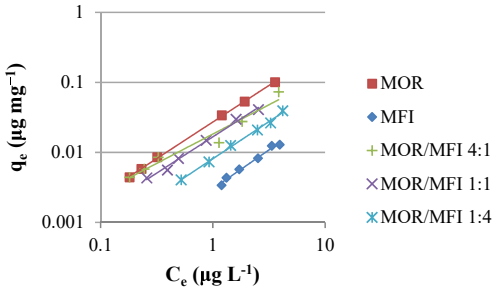

Fig. 1. Experimental adsorption isotherms for BZT adsorption in single-solute water by MOR, MFI and zeolite mixtures.

Table 3
The Freundlich model constants for BZT adsorption in single-solute water by MOR, MFI and zeolite mixtures.

Constant [a]	MOR	MFI	MOR/MFI 4:1	MOR/MFI 1:1	MOR/MFI 1:4
n	1.02	1.11	0.84	1.03	1.06
$K_F \times 10^3$	24.4	3.0	18.3	16.7	8.1
R^2	0.95	0.98	0.95	0.99	0.99

[a] The unit of K_F is $(\mu g\ mg^{-1})\ (\mu g\ L^{-1})^{-n}$.

ities by zeolite mixtures from the known adsorption isotherms of single zeolites. In this study, a predicted adsorption isotherm of OMPs by zeolite mixtures (calculated isotherm) was calculated according to the adsorption isotherms of single zeolites from the experiment (experimental isotherm) and the mass ratios of single zeolites, as shown in Eq. (3),

$$q_{e,Mix} = Massratio_{MOR} \times K_{FMOR} C_e^{nMOR} + Massratio_{MFI} \times K_{FMFI} C_e^{nMFI} \quad (3)$$

where K_{FMOR} ($(\mu g\ mg^{-1})\ (\mu g\ L^{-1})^{-n}$) and n_{MOR} (-) are the Freundlich constants of MOR, K_{FMFI} ($(\mu g\ mg^{-1})\ (\mu g\ L^{-1})^{-n}$) and n_{MFI} (-) are the Freundlich constants of MFI, Mass $ratio_{MOR}$ and Mass $ratio_{MFI}$ are the mass ratios of MOR and MFI in zeolite mixture, respectively. For example, when OMP was removed by MOR/MFI 4:1, Mass $ratio_{MOR}$ and Mass $ratio_{MFI}$ were 0.8 and 0.2, respectively.

Calculated isotherms were listed in Table S4 and their accuracies were evaluated in Fig. 2. As can be seen, experimental isotherm data of mixed high-silica zeolite adsorption were close to calculated isotherms and the deviations were almost in ±20%. This phenomenon indicated that in single-solute water, the adsorption capacity of BZT by the mixture of MOR and MFI was as expected well described by the adsorption isotherms of single zeolites in proportion to their mass ratios.

3.2. Adsorption of BZT in multi-solute water

The adsorption of BZT in multi-solute water by MOR, MFI and their mixtures was investigated. The obtained adsorption isotherm data were fitted by the Freundlich model, as shown in Fig. 3. The Freundlich model constants were listed in Table 4. Similar to the adsorption of BZT in single-solute water, in multi-solute water, adsorption capacity of BZT by zeolite mixtures decreased with the increase of MFI mass ratio. The affinity between MOR and BZT (K_F = 20.4E-3) was stronger than that between MFI and BZT (K_F = 2.2E-3).

The adsorption capacities of BZT by MOR, MFI and their mixtures in single-solute water and multi-solute water were compared in Fig. 4. The ±20% deviation lines were plotted based on the isotherms obtained in single-solute water. Single zeolites and zeolite mixtures showed lower adsorption capacity for BZT in multi-solute water than in single-solute

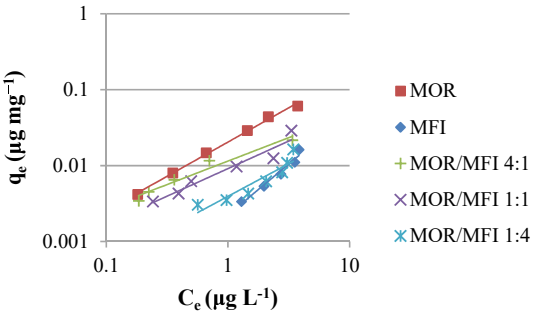

Fig. 3. Experimental adsorption isotherms for BZT adsorption in multi-solute water by MOR, MFI and zeolite mixtures.

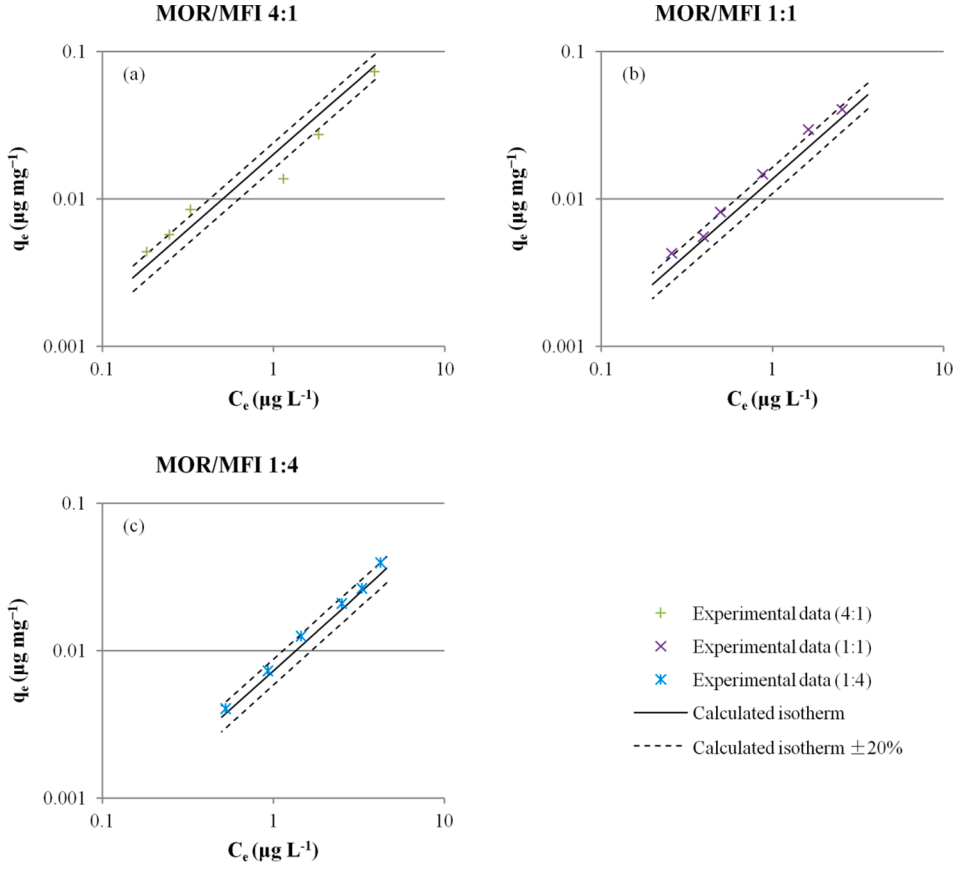

Fig. 2. Adsorption of BZT in single-solute water: Experimental adsorption isotherms by zeolite mixtures in comparison to calculated isotherms and ±20% deviation lines corresponding to calculated isotherms.

Table 4
The Freundlich model constants for BZT adsorption in multi-solute water by MOR, MFI and zeolite mixtures.

Constant [a]	MOR	MFI	MOR/MFI 4:1	MOR/MFI 1:1	MOR/MFI 1:4
n	0.90	1.34	0.62	0.72	0.86
$K_F \times 10^3$	20.4	2.2	11.4	9.1	3.9
R^2	0.99	0.96	0.96	0.94	0.87

[a] The unit of K_F is (μg mg^{-1}) (μg L^{-1})$^{-n}$.

water, which was reflected in the K_F value being lower in multi-solute water (Table 4) than in single solute water (Table 3). In multi-solute water, other OMPs might compete with BZT for available adsorption sites, leading to a decreased capacity of BZT compared with the adsorption capacity of BZT in single-solute water.

For the adsorption of BZT by MOR (Fig. 4a) and MFI (Fig. 4b), the adsorption capacities of BZT in multi-solute water were nearly within −20% range of the BZT adsorption capacities in single-solute water. In contrast, for the adsorption of BZT by MOR/MFI 1:4 (Fig. 4e), all the adsorption capacity data in multi-solute water were smaller than −20% of the data in single-solute water. And for the adsorption of BZT by MOR/MFI 4:1 (Fig. 4c) and MOR/MFI 1:1 (Fig. 4d), two and five adsorption capacity data in multi-solute water were out of −20% deviation of adsorption isotherms in single-solute water, respectively. In other words, the reduced adsorption capacity of zeolite mixtures in multi-solute water became more obvious with the increase of MFI mass ratio.

In multi-solute water, different OMPs competed for the adsorption sites on MOR and MFI, the adsorption capacity of BZT in multi-solute water thereby decreased compared to single-solute water. On top of OMP competing for adsorption sites within one zeolite, in the process of OMP adsorption by zeolite mixtures, OMPs also competed for the more-effective zeolite in zeolite mixtures. Adsorption sites on MOR were preferentially occupied by other easier adsorbed OMPs (the OMPs with higher affinity to MOR). When MOR was the minority in a zeolite mixture, BZT had to be adsorbed by MFI, which was less effective than MOR, thus the decrease of adsorption capacity was much more obvious.

In multi-solute water, adsorption isotherms of BZT by zeolite mixtures were calculated from the experimental adsorption isotherms of BZT by MOR and MFI zeolites. The results were shown in Table S5. The calculated and experimental adsorption isotherms of zeolite mixtures were compared in Fig. 5.

As shown in Fig. 5a and 5b, four experimental data from MOR/MFI 4:1 and three experimental data from MOR/MFI 1:1 were ranged in ±20% deviation of calculated isotherms. For the adsorption by MOR/MFI 1:4 (Fig. 5c), all the experimental data were smaller than values from calculated isotherm and six out of seven experimental data fell out of −20% deviation of calculated isotherm. The deviation between experimental isotherm and calculated isotherm became more obvious with higher mass ratio of MFI, which was less efficient than MOR for BZT adsorption. With the competition of other OMPs in multi-solute water, adsorption isotherms of BZT by zeolite mixtures were calculated with less accuracy by solely combining experimental isotherms of single zeolites, especially when the less-effective zeolite, e.g., MFI, was dominant in the mixture. The possible mechanism would be further discussed in Section 3.3.

3.3. Adsorption of other OMPs in multi-solute water

The adsorption of MBZ, CBZ, DCF, MTP, SMX, PRO and STL by zeolites (mixtures) was studied. The removal efficiencies of OMPs by MOR, MFI and zeolite mixtures were summarized in Table 5.

Positively charged MTP, PRO and STL were completely removed by MOR and zeolite mixtures, even at a very low dosage. The results of zeta potential measurement show that, at experimental pH value of ~5.8, the overall charges at the external surface of MOR and MFI zeolites were negative and the net charge increased with pH (Figure S2). Due to the deionization of hydrogen atoms from the framework of MOR and MFI zeolites, there were negatively charged sites formed at the surface of zeolites [29]. Positively charged OMPs in the solution would experience the electrostatic attraction with negative charged external surface of zeolites and easily diffused into the micropores. Since the external surface and internal micropores of zeolites accounted for 16% and 84% of total BET surface area, respectively, a majority of OMPs will be adsorbed in the internal pores of zeolites. The adsorption capabilities of MFI towards PRO and STL were lower than the capabilities of MOR. One possible reason for this was that MOR with a lower zeta potential than MFI could provide more negatively charged sites to positively charged

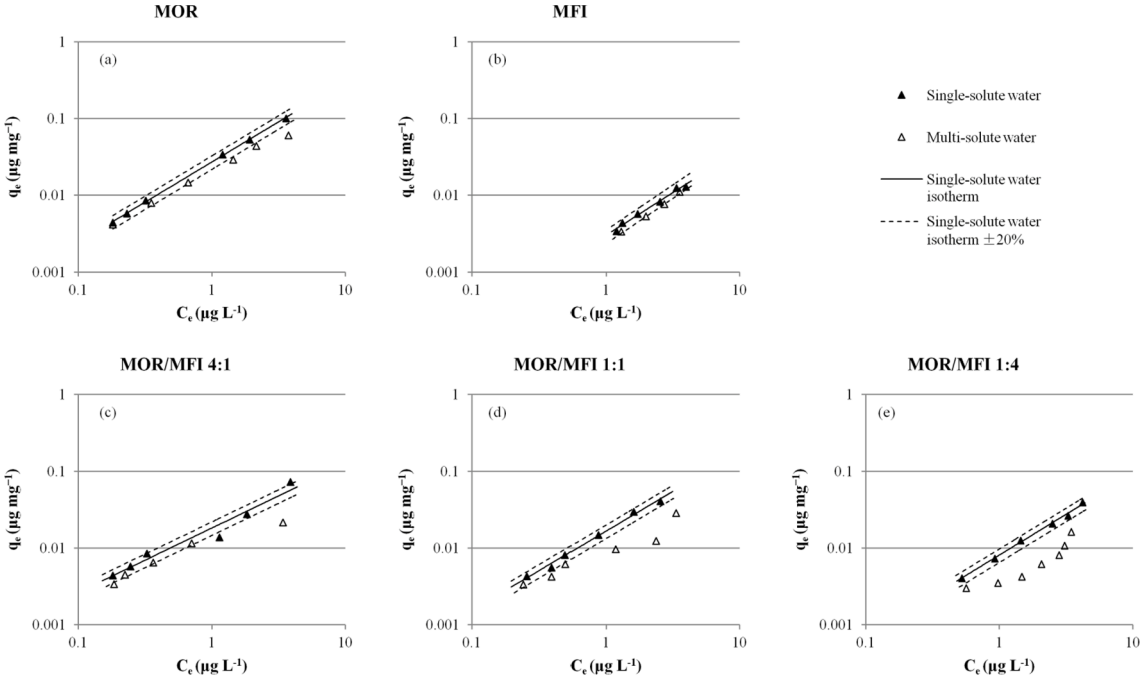

Fig. 4. Adsorption isotherms of BZT in single-solute water and in multi-solute water by (a) MOR, (b) MFI, (c) MOR/MFI 4:1, (d) MOR/MFI 1:1 and (e) MOR/MFI 1:4.

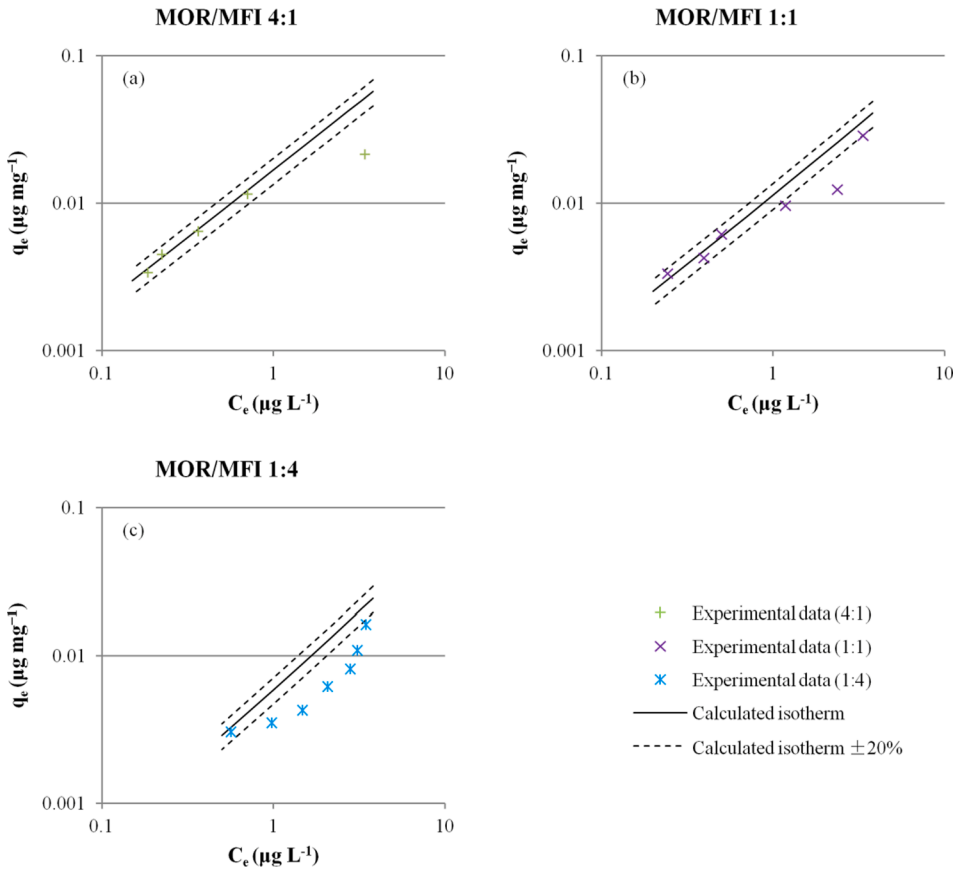

Fig. 5. Adsorption of BZT in multi-solute water: Experimental adsorption isotherms by zeolite mixtures in comparison to calculated isotherms and ±20% deviation lines corresponding to calculated isotherms.

Table 5
The Freundlich model constants for OMP adsorption in multi-solute water by MOR, MFI and zeolite mixtures.

OMPs	Surface charge [c]	Constant [d]	MOR	MFI	MOR/MFI 4:1	MOR/MFI 1:1	MOR/MFI 1:4
Metoprolol (MTP)	+	n	Complete removal [b]	Complete removal [b]	Complete removal [b]	Complete removal [b]	Complete removal [b]
		$K_F \times 10^3$					
		R^2					
Propranolol (PRO)	+	n	Complete removal [b]	0.55	Complete removal [b]	Complete removal [b]	Complete removal [b]
		$K_F \times 10^3$		65.7			
		R^2		0.96			
Sotalol (STL)	+	n	Complete removal [b]	1.06	Complete removal [b]	Complete removal [b]	Complete removal [b]
		$K_F \times 10^3$		784.0			
		R^2		0.98			
Diclofenac (DCF)	–	n	Low removal [a]	Low removal [a]	Low removal [a]	Low removal [a]	Low removal [a]
		$K_F \times 10^3$					
		R^2					
Sulfamethoxazole (SMX)	–	n	1.00	1.05	0.61	0.84	0.88
		$K_F \times 10^3$	23.6	49.7	12.7	24.2	28.7
		R^2	0.94	0.99	0.94	0.97	0.99
5-methyl-benzotriazole (MBZ)	0	n	1.01	5.49	0.86	0.62	0.75
		$K_F \times 10^3$	117.7	0.1	62.6	26.4	13.6
		R^2	0.99	0.93	0.94	0.95	0.81
Carbamazepine (CBZ)	0	n	0.67	Low removal [a]	0.76	0.80	0.70
		$K_F \times 10^3$	20.3		14.0	9.0	4.2
		R^2	0.95		0.99	0.99	0.97

[a] Removal percentage was lower than 15% when the high-silica zeolite dosage was 1000 mg L^{-1}.
[b] Removal percentage was higher than 98% when the high-silica zeolite dosage was 10 mg L^{-1}.
[c] The surface charge of OMPs at pH 5.8.
[d] The unit of K_F is (μg mg^{-1}) (μg L^{-1})$^{-n}$.

PRO and STL. Furthermore, the higher adsorption capabilities of MOR towards PRO and STL may also benefit from MOR's larger surface area and pore volume.

On the other hand, negatively charged DCF, with the highest molecular weight (MW = 296.1 g mol^{-1}) among all the investigated OMPs, was the most hardly removed by MOR, MFI and zeolite mixtures.

Generally, OMP with a higher molecular weight has a larger molecular size. Possibly DCF was too large to diffuse into the pores and to reach the inner adsorption sites of high-silica zeolites, therefore leading to a bad removal performance. In addition, the negatively charged OMPs would experience electrostatic repulsion with the negatively charged surface of zeolites, which may hinder their adsorption.

BZT and MBZ were neutral OMPs with a similar chemical structure and close molecular weight. By referring to K_F value, MBZ was better adsorbed by MOR ((K_F = 117.7E-3) than BZT (K_F = 20.4E-3). MBZ with one additional methyl group to BZT was more hydrophobic than BZT, thus provided a better affinity to MOR by hydrophobic interaction, which was a strong attraction between hydrophobic molecules and surfaces in water [33]. The effect of surface charge of zeolites on the adsorption of neutral OMPs would be negligible.

The hydrophobicity of zeolites is decided by their Al content: Zeolites with less Al are more hydrophobic [34,35]. In this study, MFI zeolite with higher Si/Al ratio and lower number of acid sites (Table 1) was supposed to be more hydrophobic than MOR zeolite, However, as shown in Table 3, the adsorption efficiencies of seven out of eight OMPs on MFI were lower than that of MOR zeolite, indicating the minimal effect of zeolites' hydrophobicity on the adsorption efficiencies of OMPs. In previous studies, the maximum adsorption capacity of organic pollutants at the equilibrium concentration range of mg L^{-1} on zeolites was higher, when zeolites with higher Si/Al ratio were applied as adsorbents [24,36,37]. In our study, the obtained adsorption capacity of OMPs at several μg L^{-1} was much lower than the maximum adsorption capacity. Since the adsorption sites on zeolites were sufficient for both OMP and water molecules, the effect of zeolites' hydrophobicity on OMP adsorption at the range of μg L^{-1} could be negligible.

Overall, the adsorption process of OMPs by high-silica zeolites was affected by the physicochemical properties of OMPs, e.g., charge, hydrophobicity and molecular size, as well as by the characteristics of high-silica zeolites, e.g., pore size and surface charge. The adsorption mechanisms of OMP adsorption by high-silica zeolites included electrostatic interaction and hydrophobic interaction.

The adsorption of 16 OMPs with initial concentration of 2 μg L^{-1} in demineralized water on MOR and MFI zeolites has been studied by de Ridder et al. [28]. Metoprolol was completely removed by MOR and MFI zeolites, while both zeolites had limited removal for sulfamethoxazole. Carbamazepine was hardly removed by MFI and partially removed by MOR. The finding in the literature was consistent with the results in our study. Rossner et al. [27] investigated the removal of 25 OMPs with initial concentrations of 200 – 900 ng L^{-1} in surface water by zeolites, activated carbon and carbonaceous resin. MOR zeolite removed 15 out of 25 OMPs, including trimethoprim and carbamazepine, while only three OMPs were removed by FAU zeolite. All tested OMPs were partially or completely removed by carbonaceous resin and activated carbon. It has been proved that zeolites with homogeneous pore size and shape were effective for a limited range of OMPs.

The experimental adsorption isotherms of SMX, CBZ and MBZ by zeolite mixtures were obtained (Table 5) and compared with the calculated isotherms in Figs. 6, 7 and Figure S5, respectively. As shown in Fig. 6, experimental isotherm data of SMX adsorption by zeolite mixtures were lower than the calculated isotherm values, and less deviations were observed with the increased mass ratio of MFI, which had better SMX adsorption efficiency than MOR. The same phenomenon was observed in the adsorption of BZT (Fig. 5) and MBZ (Figure S5), demonstrating that more deviation of calculated isotherm was observed when less efficient zeolite became dominant in the zeolite mixture.

Fig. 6a shows that four data points from the isotherm of MOR/MFI 4:1 at higher zeolite dosages (lower equilibrium concentrations) were close to the isotherm of MOR, while the other three data points at lower zeolite dosages (higher equilibrium concentrations) fell below the isotherm of MOR. In this study, SMX was the only negatively charged OMP with adsorption isotherms on two single zeolites and three zeolite mixtures. As shown in Table 5, positively charged OMPs were preferably adsorbed on MOR zeolite, which may hinder the adsorption of SMX. The channel of MOR can be blocked by one positively charged OMP molecule, which will further shield the adsorption sites in the channel. At lower dosage of zeolite mixture, the competition of positively charged OMPs with SMX would be more severe and the adsorption capacity of SMX on MOR might completely lose. Notably, SMX was partially adsorbed on single MOR zeolite (Fig. 6a), indicating the adsorption capacity of SMX on single MOR remained. The interesting phenomenon is worth well further investigation.

Fig. 7 reveals that experimental isotherm data of CBZ adsorption by

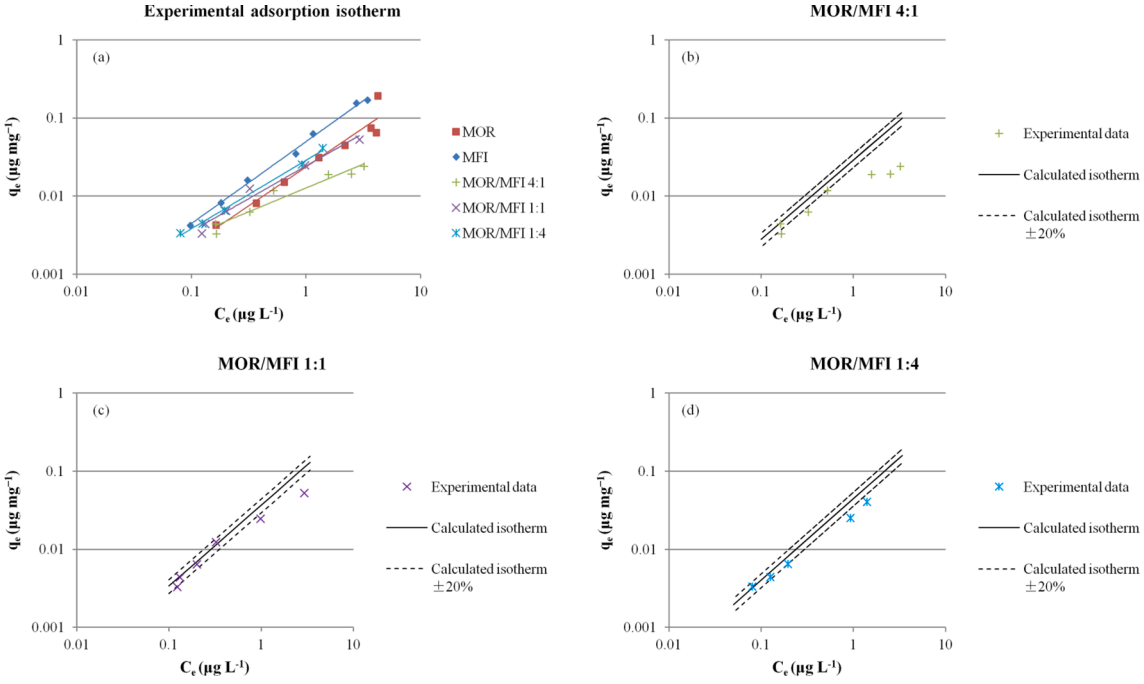

Fig. 6. Adsorption of SMX in multi-solute water: (a) Experimental adsorption isotherms by MOR, MFI and zeolite mixtures with the Freundlich model fitting; (b)-(d) Experimental adsorption isotherms by zeolite mixtures in comparison to calculated isotherms and ±20% deviation lines corresponding to calculated isotherms.

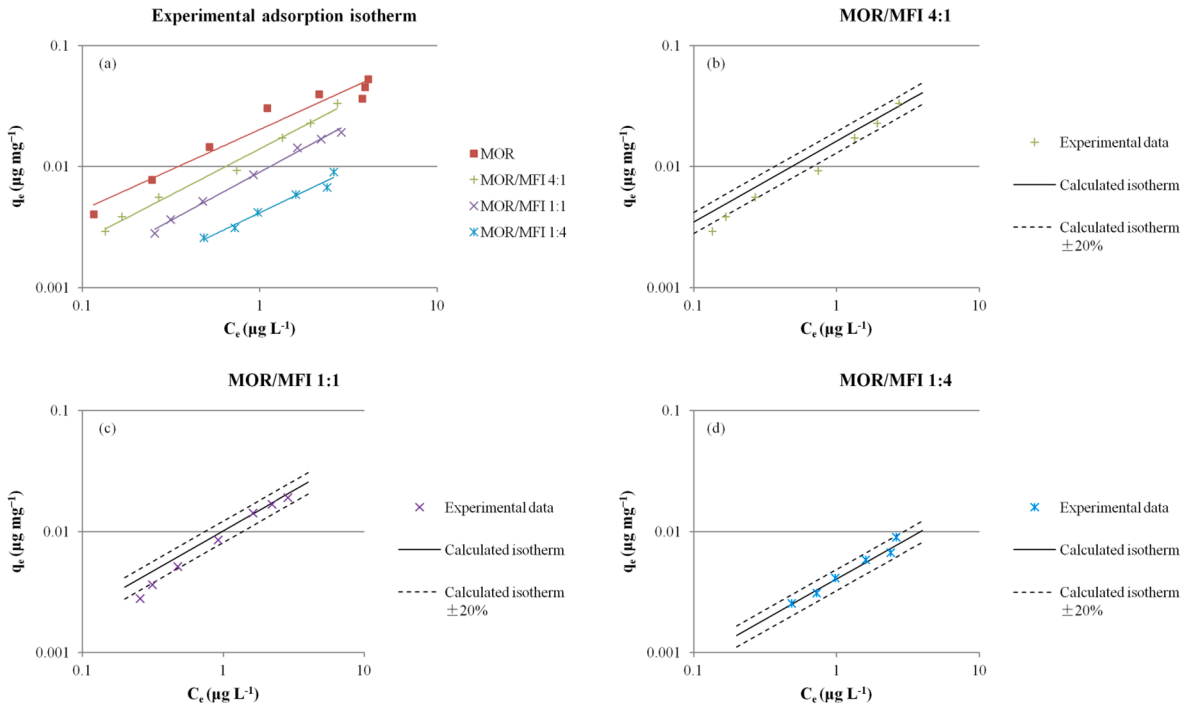

Fig. 7. Adsorption of CBZ in multi-solute water: (a) Experimental adsorption isotherms by MOR and zeolite mixtures with the Freundlich model fitting; (b)-(d) Experimental adsorption isotherms by zeolite mixtures in comparison to calculated isotherms and ±20% deviation lines corresponding to calculated isotherms.

zeolite mixtures were close to calculated isotherms and the deviations were almost within ±20%. CBZ was only adsorbed by MOR, so adding MOR and MFI mixture was equal to adding single MOR with corresponding mass ratio. In the adsorption of CBZ by zeolite mixtures, CBZ did not need to compete for the more-effective zeolite, because it could not be adsorbed by MFI. Therefore, the adsorption isotherm of CBZ by the mixture of MOR and MFI was well calculated by the experimental adsorption isotherm of MOR in proportion to MOR's mass ratio. This phenomenon observed in CBZ adsorption by zeolite mixtures also supported our above findings from another point of view, indicating that the deviation between experimental isotherm and calculated isotherm was caused by the competition for the more effective zeolite.

Due to the affinity difference towards MBZ between MOR and MFI, experimental isotherm data of MBZ were smaller than calculated isotherm values, especially when MFI was dominant in the mixture (Figure S5). This phenomenon was similar to the mixed high-silica zeolite adsorption isotherms of BZT. In the adsorption of BZT and MBZ by zeolite mixtures, these two OMPs had a chance to be adsorbed by both MOR and MFI. Although they preferred to be adsorbed by the more-effective zeolite MOR, available adsorption sites on this more-effective zeolite were preferentially occupied by other easier adsorbed OMPs, such as PRO and STL, because PRO and STL were completely removed even at the adsorption condition of MOR/MFI 1:4 (Table 5). BZT and MBZ were at a disadvantage in the competition for more-effective zeolite MOR, especially when MOR was the minority in a zeolite mixture. In this case, BZT and MBZ had to be adsorbed by MFI, which was less effective than MOR, therefore the experimental adsorption isotherm data of BZT and MBZ by zeolite mixtures were less than the calculation, and the deviation between experimental isotherm and calculated isotherm became more obvious with lower mass ratio of MOR. Another explanation could be found from the channel-shaped pores in MOR. Perhaps the adsorption of an OMP with a very high affinity to MOR blocked the channel for the adsorption of BZT and MBZ with a lower affinity and with that decreased the surface available for adsorption.

All the above findings demonstrated that in multi-solute water, with the competition for more-effective zeolite, adsorption isotherms by zeolite mixtures were harder to be calculated from experimental single isotherms with the decrease of more-effective zeolite mass ratio in MOR and MFI mixture, which was consistent with the conclusion obtained in Section 3.2.

4. Conclusions

MOR and MFI high-silica zeolites were mixed in different mass ratios and served as the adsorbents to remove BZT, MBZ, CBZ, DCF, MTP, SMX, PRO and STL from water at an environmentally relevant concentration. For the adsorption by zeolite mixtures, a broad range of OMPs achieved proper removal efficacy, while for the adsorption by single zeolite, only a narrow spectrum of OMPs was removed. In order to pre-estimate the OMP adsorption capabilities by zeolite mixtures, adsorption isotherms of OMPs on zeolite mixtures were predicted by the experimental adsorption isotherms and mass ratios of single zeolites. In single-solute water, adsorption isotherms on zeolite mixtures were well predicted by the adsorption isotherms on single zeolites in proportion to the mass ratios between single zeolites. While in multi-solute water, adsorption isotherms on zeolite mixtures were difficult to be predicted from experimental single isotherms. In multi-solute water, experimental isotherm data of zeolite mixtures were lower than the predicted values, and the deviations became more obvious with the increase of less-effective zeolite mass ratio in MOR and MFI mixture. The difference of isotherm prediction between single-solute water and multi-solute water could be explained by the competition for more-effective zeolite between different OMPs. For the adsorption by zeolite mixtures in multi-solute water, available adsorption sites on the more-effective zeolite were preferentially occupied by positively charged OMPs, which were favorably adsorbed by zeolites. Neutral and negatively charged OMPs with a lower affinity for zeolites were forced to be adsorbed on less-effective zeolite, especially when more-effective zeolite was the minority in the zeolite mixture, thereby leading to a lower adsorption efficacy than prediction.

CRediT authorship contribution statement

Xinyu Zheng: Formal analysis, Investigation, Writing – original draft. **Nan Jiang:** Writing – review & editing, Supervision, Methodology. **Huaili Zheng:** Supervision. **Yuyang Wu:** Visualization, Writing – review & editing. **Sebastiaan G.J. Heijman:** Conceptualization, Funding acquisition.

Declaration of Competing Interest

The authors declare that they have no known competing financial interests or personal relationships that could have appeared to influence the work reported in this paper.

Acknowledgments

This research was financially supported by Nederlandse Organisatie voor Wetenschappelijk Onderzoek (Netherlands Organization for Scientific Research, NWO, No. 15756). Xinyu Zheng acknowledges the China Scholarship Council for her visiting PhD scholarship under the State Scholarship Fund (No. 201906050137).

Appendix A. Supplementary material

Supplementary data to this article can be found online at https://doi.org/10.1016/j.seppur.2021.120009.

References

[1] M. Roman, L. Gutierrez, L.H. Van Dijk, M. Vanoppen, J.W. Post, B.A. Wols, E. R. Cornelissen, A.R.D. Verliefde, Effect of pH on the transport and adsorption of organic micropollutants in ion-exchange membranes in electrodialysis-based desalination, Sep. Purif. Technol. 252 (2020), 117487.
[2] M. Roman, L.H. Van Dijk, L. Gutierrez, M. Vanoppen, J.W. Post, B.A. Wols, E. R. Cornelissen, A.R.D. Verliefde, Key physicochemical characteristics governing organic micropollutant adsorption and transport in ion-exchange membranes during reverse electrodialysis, Desalination 468 (2019), 114084.
[3] N. Bolong, A.F. Ismail, M.R. Salim, T. Matsuura, A review of the effects of emerging contaminants in wastewater and options for their removal, Desalination 239 (1-3) (2009) 229–246.
[4] O.A. Jones, N. Voulvoulis, J.N. Lester, Potential impact of pharmaceuticals on environmental health, Bull. World Health Organ. 81 (2003) 768–769.
[5] J. Shin, Y.-G. Lee, S.-H. Lee, S. Kim, D. Ochir, Y. Park, J. Kim, K. Chon, Single and competitive adsorptions of micropollutants using pristine and alkali-modified biochars from spent coffee grounds, J. Hazard. Mater. 400 (2020), 123102.
[6] O. Rozas, C. Baeza, K. Núñez, A. Rossner, R. Urrutia, H.D. Mansilla, Organic micropollutants (OMPs) oxidation by ozone: Effect of activated carbon on toxicity abatement, Sci. Total Environ. 590–591 (2017) 430–439.
[7] Z. Wang, B. Zhang, C. Fang, Z. Liu, J. Fang, L. Zhu, Macroporous membranes doped with micro-mesoporous β-cyclodextrin polymers for ultrafast removal of organic micropollutants from water, Carbohydr. Polym. 222 (2019), 114970.
[8] G. Aschermann, C. Schröder, F. Zietzschmann, M. Jekel, Organic micropollutant desorption in various water matrices - Activated carbon pore characteristics determine the reversibility of adsorption, Chemosphere 237 (2019), 124415.
[9] L. Piai, J.E. Dykstra, M.G. Adishakti, M. Blokland, A.A.M. Langenhoff, A. van der Wal, Diffusion of hydrophilic organic micropollutants in granular activated carbon with different pore sizes, Water Res. 162 (2019) 518–527.
[10] J.M. Dias, M.C.M. Alvim-Ferraz, M.F. Almeida, J. Rivera-Utrilla, M. Sánchez-Polo, Waste materials for activated carbon preparation and its use in aqueous-phase treatment: A review, J. Environ. Manage. 85 (2007) 833–846.
[11] Y. Ling, M.J. Klemes, S. Steinschneider, W.R. Dichtel, D.E. Helbling, QSARs to predict adsorption affinity of organic micropollutants for activated carbon and β-cyclodextrin polymer adsorbents, Water Res. 154 (2019) 217–226.
[12] Y. Luo, W. Guo, H.H. Ngo, L.D. Nghiem, F.I. Hai, J. Zhang, S. Liang, X.C. Wang, A review on the occurrence of micropollutants in the aquatic environment and their fate and removal during wastewater treatment, Sci. Total Environ. 473-474 (2014) 619–641.
[13] K. Kosek, A. Luczkiewicz, S. Fudala-Książek, K. Jankowska, M. Szopińska, O. Svahn, J. Tränckner, A. Kaiser, V. Langas, E. Björklund, Implementation of advanced micropollutants removal technologies in wastewater treatment plants (WWTPs) - Examples and challenges based on selected EU countries, Environ. Sci. Policy 112 (2020) 213–226.
[14] N. Jiang, R. Shang, S.G.J. Heijman, L.C. Rietveld, Adsorption of triclosan, trichlorophenol and phenol by high-silica zeolites: Adsorption efficiencies and mechanisms, Sep. Purif. Technol. 235 (2020) 116152, https://doi.org/10.1016/j.seppur.2019.116152.
[15] N. Jiang, R. Shang, S.G.J. Heijman, L.C. Rietveld, High-silica zeolites for adsorption of organic micro-pollutants in water treatment: A review, Water Res. 144 (2018) 145–161.
[16] R.F. Lobo, High-silica zeolites: From synthesis to structure, Abstr. Pap. Am. Chem. Soc. 213 (1997) 345-COLL.
[17] H.-W. Hung, T.-F. Lin, C. Baus, F. Sacher, H.-J. Brauch, Competitive and hindering effects of natural organic matter on the adsorption of MTBE onto activated carbons and zeolites, Environ. technol. 26 (12) (2005) 1371–1382.
[18] X. Guo, L. Zeng, X. Jin, Advanced regeneration and fixed-bed study of ammonium and potassium removal from anaerobic digested wastewater by natural zeolite, J. Environ. Sci. 25 (5) (2013) 954–961.
[19] F. Sannino, S. Ruocco, A. Marocco, S. Esposito, M. Pansini, Cyclic process of simazine removal from waters by adsorption on zeolite H-Y and its regeneration by thermal treatment, J. Hazard. Mater. 229-230 (2012) 354–360.
[20] M. Fu, M. He, B. Heijman, J.P. van der Hoek, Ozone-based regeneration of granular zeolites loaded with acetaminophen, Sep. Purif. Technol. 256 (2021), 117616.
[21] Y. Doekhi-Bennani, N.M. Leilabady, M. Fu, L.C. Rietveld, J.P. van der Hoek, S.G. J. Heijman, Simultaneous removal of ammonium ions and sulfamethoxazole by ozone regenerated high silica zeolites, Water Res. 188 (2021), 116472.
[22] N. Jiang, M. Erdős, O.A. Moultos, R. Shang, T.J.H. Vlugt, S.G.J. Heijman, L. C. Rietveld, The adsorption mechanisms of organic micropollutants on high-silica zeolites causing S-shaped adsorption isotherms: an experimental and Monte Carlo simulation study, Chem. Eng. J. 389 (2020), 123968.
[23] R. Gonzalez-Olmos, F.-D. Kopinke, K. Mackenzie, A. Georgi, Hydrophobic Fe-zeolites for removal of MTBE from water by combination of adsorption and oxidation, Environ. Sci. Technol. 47 (5) (2013) 2353–2360.
[24] L. Damjanović, V. Rakić, V. Rac, D. Stošić, A. Auroux, The investigation of phenol removal from aqueous solutions by zeolites as solid adsorbents, J. Hazard. Mater. 184 (1-3) (2010) 477–484.
[25] V. Rakić, L. Damjanović, V. Rac, D. Stošić, V. Dondur, A. Auroux, The adsorption of nicotine from aqueous solutions on different zeolite structures, Water Res. 44 (6) (2010) 2047–2057.
[26] I. Braschi, A. Martucci, S. Blasioli, L.L. Mzini, C. Ciavatta, M. Cossi, Effect of humic monomers on the adsorption of sulfamethoxazole sulfonamide antibiotic into a high silica zeolite Y: An interdisciplinary study, Chemosphere 155 (2016) 444–452.
[27] A. Rossner, S.A. Snyder, D.R.U. Knappe, Removal of emerging contaminants of concern by alternative adsorbents, Water Res. 43 (15) (2009) 3787–3796.
[28] D.J. de Ridder, J.Q.J.C. Verberk, S.G.J. Heijman, G.L. Amy, J.C. van Dijk, Zeolites for nitrosamine and pharmaceutical removal from demineralised and surface water: Mechanisms and efficacy, Sep. Purif. Technol. 89 (2012) 71–77.
[29] N. Jiang, High-silica Zeolites as Novel Adsorbents for the Removal of Organic Micro-pollutants in Water Treatment, Delft University of Technology, 2019.
[30] Y. He, H. Cheng, Degradation of N-nitrosodimethylamine (NDMA) and its precursor dimethylamine (DMA) in mineral micropores induced by microwave irradiation, Water Res. 94 (2016) 305–314.
[31] A. Erdem-Şenatalar, J.A. Bergendahl, A. Giaya, R.W. Thompson, Adsorption of methyl tertiary butyl ether on hydrophobic molecular sieves, Environ. Eng. Sci. 21 (6) (2004) 722–729.
[32] D.R.U. Knappe, A.A.R. Campos, Effectiveness of high-silica zeolites for the adsorption of methyl tertiary-butyl ether from natural water, Water Sci. Technol. Water Supply 5 (2005) 83-91.
[33] J.N. Israelachvili, Intermolecular and Surface Forces, third ed., Academic Press, Boston, 2011, pp. 151–167.
[34] N.Y. Chen, Hydrophobic properties of zeolites, J. Phys. Chem. 80 (1976) 60–64.
[35] D.H. Olson, W.O. Haag, W.S. Borghard, Use of water as a probe of zeolitic properties: interaction of water with HZSM-5, Micropor. Mesopor. Mat. 35-36 (2000) 435–446.
[36] M.A. Anderson, Removal of MTBE and other organic contaminants from water by sorption to high silica zeolites, Environ. Sci. Technol. 34 (4) (2000) 725–727.
[37] A.H. Yonli, I. Batonneau-Gener, J. Koulidiati, Adsorptive removal of alpha-endosulfan from water by hydrophobic zeolites. An isothermal study, J. Hazard. Mater. 203 (2012) 357–362.